Current Research in Toxicology 7 (2024) 100200

Contents lists available at ScienceDirect

Current Research in Toxicology

journal homepage: www.journals.elsevier.com/current-research-in-toxicology

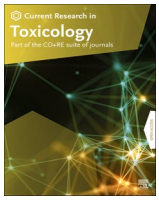

Research Paper

Estrogen replacement therapy reverses spatial memory loss and pyramidal cell neurodegeneration in the prefrontal cortex of lead-exposed ovariectomized Wistar rats

Abiodun Shukrat Lasisi-Sholola [a,b], Sodiq Opeyemi Hammed [a], Richard Adedamola Ajike [a], Roland Eghoghosoa Akhigbe [a,b], Oladele Ayobami Afolabi [a,*]

[a] Department of Physiology, Ladoke Akintola University of Technology, Ogbomoso, Oyo State, Nigeria
[b] Reproductive Biology and Toxicology Research Laboratory, Oasis of Grace Hospital, Osogbo, Osun State, Nigeria

ARTICLE INFO

Keywords:
Cognition
Heavy metals
Hormone replacement therapy
Lead
Memory
Estrogen

ABSTRACT

Background: Although menopause is a component of chronological aging, it may be induced by exposure to heavy metals like lead. Interestingly, lead exposure, just like the postmenopausal state, has been associated with spatial memory loss and neurodegeneration; however, the impact of hormone replacement therapy (HRT) on menopause and lead-induced spatial memory loss and neurodegeneration is yet to be reported.
Aim: The present study investigated the effect and associated mechanism of HRT on ovariectomized-driven menopausal state and lead exposure-induced spatial memory loss and neurodegeneration.
Materials and methods: Thirty adult female Wistar rats were randomized into 6 groups (n = 5 rats/group); the sham-operated vehicle-treated, ovariectomized (OVX), OVX + HRT, lead-exposed, OVX + lead, and OVX + Lead + HRT groups. Treatment was daily via gavage and lasted for 28 days.
Results: Ovariectomy and lead exposure impaired spatial memory deficit evidenced by a significant reduction in novel arm entry, time spent in the novel arm, alternation, time exploring novel and familiar objects, and discrimination index. These findings were accompanied by a marked distortion in the histology of the prefrontal cortex, and a decline in serum dopamine level and pyramidal neurons. In addition, ovariectomy and lead exposure induced metabolic disruption (as depicted by a marked rise in lactate level and lactate dehydrogenase and creatinine kinase activities), oxidative stress (evidenced by a significant increase in MDA level, and decrease in GSH level, and SOD and catalase activities), inflammation (as shown by significant upregulation of myeloperoxidase activity, and TNF-α and IL-1β), and apoptosis (evidenced by a rise in caspase 3 activity) of the prefrontal cortex. The observed biochemical and histological perturbations were attenuated by HRT.
Conclusions: This study revealed that HRT attenuated ovariectomy and lead-exposure-induced spatial memory deficit and pyramidal neurodegeneration by suppressing oxidative stress, inflammation, and apoptosis of the prefrontal cortex.

1. Introduction

Menopause is a crucial stage in the life of women which often starts as temporary then develops into permanent cessation of the activities of the ovarian follicles, leading to discontinuation in the menstrual cycle (Santoro et al., 2021; Ellington et al., 2022). Although menopause is a component of the aging woman, it may also be triggered by other factors such as chemotherapy, ovariectomy, and exposure to heavy metals such as lead (Levine and Hall, 2023). Menopause is characterized by an increase in follicle-stimulating hormone (FSH) and luteinizing hormone (LH) levels (Giannini et al., 2021; Ambikairajah et al., 2022) and a decline in inhibin B (Goney et al., 2020; Tanbo and Fedorcsak, 2021), estrogen and progesterone levels (Zhang et al., 2020). It is also associated with an increase in free radical generation due to a decline in the levels of estrogen, which is a natural antioxidant (Sabbatini and Kararigas, 2020; Cheng et al., 2021).

Exposure to heavy metals like lead may hasten the onset of menopause and/or worsen the complications of menopause. Exposure occurs

* Corresponding author.
E-mail address: aoafolabi59@lautech.edu.ng (O.A. Afolabi).

https://doi.org/10.1016/j.crtox.2024.100200
Received 29 May 2024; Received in revised form 16 October 2024; Accepted 29 October 2024
Available online 5 November 2024

majorly through occupational or environmental toxicants, lifestyle habits like smoking, dietary sources, and cosmetics use (Witkowska et al., 2021). Lead (Pb) penetrates the blood–brain-barrier (BBB) via DMT1 and calcium transporters, binds with a high binding affinity to voltage-gated calcium channels within the presynaptic neuron, and reduces the transport of calcium ions (Virgolini and Aschner, 2021), then disrupts the release of neurotransmitters like dopamine, and ultimately reduces the activation of postsynaptic receptors (Ortega et al., 2021). Increased lead concentration may also produce lead- N-methyl-D-aspartate (Pb–NMDA) complexes, leading to the disruption of intracellular Ca2 + levels in the postsynaptic neurons (Gudadhe et al., 2024), thus downregulating the release of neurotransmitters. Additionally, the production of kynurenic acid in astrocytes, heightened by Pb exposure, contributes to long-term potentiation dysfunction (Ortega et al., 2021), which may culminate in the inactivation of postsynaptic receptors and reduction in neurotransmitter release. Ultimately, Pb disrupts the cellular redox environment, fostering an oxidative milieu that promotes cell death (Ortega et al., 2021; Bjørklund et al., 2024).

Estrogen exerts anti-oxidant effects by suppressing 8-hydroxylation of guanine DNA bases (Bustamante-Barrientos et al., 2021; Bu et al., 2024), thus preventing oxidative DNA damage. However, when estrogen levels are low as seen in menopause, it exerts pro-oxidant effects due to the presence of catechol in its chemical structure which causes breakage in genetic material, forming adducts of DNA and bases oxidation (Chainy and Sahoo, 2020), leading to oxidative injury. Furthermore, T-cell activation and mediators of inflammation like tumor necrosis factor-α (TNF-α) and interleukins are markedly raised in postmenopausal women (Mohamad et al., 2020; Xu et al., 2022), indicating that menopause is accompanied by oxidative stress and inflammation (Wang et al., 2020; Iantomasi et al., 2023). The pro-oxidative and inflammatory state explains the rise in neurodegenerative diseases observed in menopausal women (Hammond et al., 2019), which is usually improved by hormone replacement therapy (Jee et al., 2021; Vrachnis et al., 2021).

Neurodegenerative diseases are a spectrum of conditions characterized by the progressive decline in movement and cognitive function and altered behavioral patterns due to the degeneration of neurons. The neuronal loss is due to neuroinflammation, oxidative stress, misfolding of proteins, and apoptosis (Kurtishi et al., 2019; Schirinzi et al., 2020). Cognition is modulated by the dopaminergic system through the fronto-striatal pathway (London, 2020; Hirano, 2021). The alterations in the dopaminergic pathway of the frontal lobe account for the cognitive decline during the process of aging (Chaudhary et al., 2021) through the downregulation of dopamine and dopaminergic receptors (Taylor et al., 2022).

Hormone replacement therapy (HRT) has been established to alleviate menopausal symptoms. However, data on the impact of HRT on cognition are conflicting. Some studies revealed that HRT did not significantly improve cognitive function in post-menopausal women (Stute et al., 2021; Andy et al., 2024; Nunes et al., 2024), while others demonstrated a significant benefit in a menopausal state induced by aging (Stute et al., 2021) and ovariectomy-induced menopause (Sharma et al., 2023). HRT has been shown to increase the level of estrogen thereby boosting anti-inflammatory and anti-oxidant defence mechanisms and conferring neuroprotection (Echeverria et al., 2021).

However, the effect and mechanism of lead exposure on cognitive function in the menopausal state, and the impact of HRT on cognition in the menopausal state with lead exposure is yet to be reported. Therefore, this study evaluated the effect of estrogen replacement therapy on cognition and pyramidal cell neurons in the prefrontal cortex of ovariectomized Wistar rats with or without lead exposure.

2. Materials and methods

2.1. Animals and treatments

The study complies with the National Institute of Health guideline regarding the use and care of laboratory animals, and it is presented in accordance with the ARRIVE guidelines. The Ethical Review Committee of Ladoke Akintola University's Faculty of Basic Medical Sciences in Nigeria gave its approval to the study protocol (ERCFBMSLAUTECH: 042/06/2024).

Thirty 12-week old female Wistar rats of about 150–200 g were used in this study. The animals were kept in clean plastic cages (5 rats per cage) in a well-ventilated room under natural conditions of 12-hour light/dark cycle and were subjected to humane care throughout the study duration. Animals were fed standard rat pellets (Breedwell Feeds; from Breedwell Feeds Ltd., Oluyole, Ibadan, Oyo State, Nigeria) and supplied with clean drinking water *ad libitum*. Animals were acclimatized for 14 days, then randomized into 6 groups (5 rats per group). Rats in the sham group were sham-operated and vehicle-treated, the ovariectomized (OVX) group underwent ovariectomy and vehicle treatment, the OVX + HRT group was ovariectomized and treated with 1.0 μg/kg b.w of ethinyloestradiol and 5.0 μg/kg b.w of levonorgestrel, lead-exposed rats were sham-operated and treated with 20 mg/kg b.w of lead acetate, OVX + lead group was ovariectomized and treated with 20 mg/kg b.w of lead acetate, and OVX + Lead + HRT rats were ovariectomized and treated with 20 mg/kg b.w of lead acetate and 1.0 μg/kg b.w of ethinyloestradiol and 5.0 μg/kg b.w of levonorgestrel. Treatments were daily by gavage and lasted for 28 days. The dose, route of administration, and duration of exposure of lead acetate are as earlier reported Besong et al. (Besong et al., 2023a), Besong et al. (Besong et al., 2023b), while the dose and route of administration of HRT were also as earlier reported (Adeyanju et al., 2018). Animals in all groups drank the same water and were kept in similar cages and bedding materials; hence there was no variation in estrogen and lead exposure apart from our administrations. The study protocol is shown in Table 1.

Table 1
Treatment protocol in the various groups.

Groups	Treatments
Sham	Sham operation + 0.2 mL of distilled water + 0.2 mL of olive oil
Ovx	Ovariectomy + 0.2 mL of distilled water + 0.2 mL of olive oil
Ovx + HT	Ovariectomy + (1.0 μg/kg b.w of ethinyl oestradiol + 5.0 μg/kg of levonorgestrel dissolved in + 0.2 mL of olive oil) + 0.2 mL of distilled water
Pb	Sham operation + 20 mg/kg b.w of lead acetate in 0.2 mL of distilled water + 0.2 mL of olive oil
Ovx + Pb	Ovariectomy + 20 mg/kg b.w of lead acetate in 0.2 mL of distilled water + 0.2 mL of olive oil
Ovx + Pb + HT	Ovariectomy + 20 mg/kg b.w of lead acetate in 0.2 mL of distilled water + (1.0 μg/kg b.w of ethinyl oestradiol + 5.0 μg of levonorgestrel dissolved in + 0.2 mL of olive oil)

Lead acetate and HRT solutions were prepared daily as required throughout the experimental period. The required dose for each rat was dissolved in 0.2 mL of distilled water and then administered to the rat via gavage. The animals were weighed daily for accurate dose calculation.

2.2. Procedure for sham operation and ovariectomy

Before the surgery, the animals were fasted for 24 h and the abdominal region was shaved. Each rat was anesthetized with an intraperitoneal injection of 50 mg/kg of ketamine and 25 mg/kg of xylazine. A lower longitudinal abdominal incision, 3 cm long, was made on the skin after cleaning the shaved area with chlorhexidine solution (Afolabi et al., 2022). The incision was developed into the peritoneal cavity. The bladder was located and mobilized to expose the uterus located posterior to the bladder. The fallopian tubes and ovaries on either side of the uterus were located and separated from the surrounding tissues. The fallopian tubes were doubled-clamped at the fimbriae end, 1 cm apart, and severed between the clamps to excise the ovary, then the loose end of each fallopian tube was sutured with vicryl 2/0. Afterward, the remaining part of the fallopian tubes were returned

into the peritoneum. The incision was closed with vicryl 2/0 and the incision site was cleaned with 10 % povidone-iodine (Afolabi et al., 2022). The same procedure was followed during the sham operation but the uterine horns were only taken out of the abdomen and returned intact. Treatment and administration commenced 24 h post-surgery.

The animals were made to rest in clean plastic cages with clean and dry bedding post-surgery. The suture sites were cleaned with 10 % povidone iodine and procaine penicillin powder applied every day to prevent infection until the sutures fell off and the wounds healed. Beddings were changed twice daily to prevent dampness which may increase susceptibility to infections.

2.3. Assessment of spatial memory and cognition using Y maze and novel object recognition

Y maze and novel object recognition (NOR) were employed to assess spatial memory and cognition. Learning and memory were evaluated using the Y maze task as previously reported (Kang et al., 2023), employing a Y maze device consisting of three arms labelled A, B, and C, with each arm measuring 35 cm in length, a height of 25 cm, and 10 cm width. Each rat was positioned at the end of one arm and permitted to liberally navigate through the maze for 5 min after a training session. Entry into an arm was recorded when all paws of the rat were fully within the arm. The number of times and duration of arm entry were observed and the percentage of obtained and recorded. Spontaneous alternation behaviour, defined as the tendency to enter into different arms successively, was used as an indicator of spatial working memory, a type of short-term memory, and also reported in percentage.

Novel object recognition was conducted as reported by Kang et al. (Kang et al., 2023). Rats were acclimated to the test environment without any objects for one hour on the day before testing was done. On the testing day, animals underwent an additional 3-minute familiarization period and were then returned to their home cages for 1 min before being placed into the observation area for the test. During this test trial, the rats explored two identical objects for 5 min, after which one of the two objects was replaced by a similar but novel object. The exploring time for the novel (N) and familiar (F) objects were recorded respectively. The discrimination index was obtained as (N-F)/ (N + F). Between experiments, the arena and objects were thoroughly cleaned with 70 % ethanol to eliminate olfactory recognition. Neurobehavioral patterns were captured by a camcorder and viewed later for scoring.

2.4. Sacrifice and sample collection

The weight of each rat was determined and then the rat was euthanized with 50 mg/kg intraperitoneal ketamine. Blood samples were obtained into plain Eppendorf bottles using a retroorbital puncture technique and the serum was collected by centrifuging the blood samples. The serum was then kept at 4 °C until it was required for the biochemical assays. The brain of each rat was removed, and the prefrontal cortex was carefully separated and dissected into the right and left hemispheres. The right hemisphere of each rats was homogenized in a cold, phosphate-buffered solution (1: 5) using a glass homogenizer. After centrifuging the homogenates at 10,000 g for 15 min at 4 °C, the supernatant was obtained and kept at 20 °C until it was required for biochemical experiments, while the left hemisphere was fixed in 10 % formosaline for histopathological processing. All laboratory assays were carried out within 6 h after sacrifice.

2.5. Biochemical assays

Lead concentrations in serum and pre-frontal cortex tissues were analyzed following the method earlier reported (Zhang et al., 2021). Specifically, a mixture of approximately 0.6 mL of 30 % H_2O_2 and 2.4 mL of 65 % HNO3 was prepared. Subsequently, 500 μL of serum or 100 mg of prefrontal cortex tissue was added to this mixture and allowed to digest at room temperature for over 12 h. The mixture was subjected to heat at 150 °C until it became clear and transparent. The volume of the solution was adjusted to 2 mL by adding 0.5 % HNO_3. The same process was repeated using blank reagents. Lead concentrations in the supernatants were determined using a flame atomic absorption spectrophotometer at 283.3 nm.

The circulating level of estrogen was assessed via spectrophotometry employing ELISA kits from Monobind Inc., USA, in accordance with the manufacturer's instructions. The determination of serum estrogen involved dispensing 25 μL of standards, controls, and serum samples into their respective wells. Subsequently, 50 μL of E2 Biotin reagent was added to all wells, followed by incubation for 30 min at 37 °C. After this incubation period, 50 μL of enzyme conjugate was added to each well, with the exception of well A1, which was reserved for the substrate blank. The wells were then covered with foil and incubated for 90 min at room temperature. Following the incubation period, the foil was removed, and the contents of the wells were aspirated. The wells were washed three times with 300 μL of diluted wash solution, with each wash cycle allowing for a soak time of more than 5 s. Any remaining fluid was carefully removed by tapping the strips on tissue paper. Subsequently, 100 μL of TMB substrate was added to all wells, and the wells were incubated in the dark at 37 °C for 30 min. Following this incubation, 50 μL of stop solution was dispensed into all wells in the same order and time interval as the substrate addition. The absorbance of the specimen was then read at 450 nm within 20 min after the addition of the stop solution to determine the levels of estrogen in the serum samples.

Dopamine concentration, a neurotransmitter which is used as an index of neurodegeneration was assayed for using an ELISA kit (Abnova, UK) following the manufacturer's guidelines. An appropriate volume of dopamine solution and a certain amount of NaHCO3 solution were added to a 10 mL colorimetric tube to ensure that the final pH of the mixture solution was 8.5. The colour of the mixture solution turned pale yellow at room temperature after a certain time, which was light green under ultraviolet lamp. Then, the fluorescence intensity of the mixture solution was measured by the fluorescence spectrophotometer, and the dopamine concentration was measured by further calculation. The novel dopamine detection method does not need any fluorescent substances in the test solution, and it further reduces the experimental error and simplifies the experimental operation procedure. The pH of the solution is an important factor for the experiment. After adding dopamine solution and NaHCO3 solution, the pH value of the mixture solution must be regulated to 8.5 by adjusting the amount of NaHCO3 solution. As shown in Fig. 2, the dopamine oxidised to a quinone derivative under alkaline condition. At the same time, the quinone derivative was unstable under alkaline condition and rapidly polymerised to form PDA nanoparticles. And then DA concentration could be detected by the fluorescence intensity of the PDA nanoparticles.

Ellman's method was employed to determine the activity of acetylcholinesterase (AchE). A disposable cuvette was consequently filled with 0.4 mL of 0.4 mg/mL DTNB, 25 μL of AChE solution (0.5 μkat in 1 mM acetylthiocholine), 425 μL of PBS, 50 μL of paraoxon in isopropanol or isopropanol alone. The reaction was started by adding 100 μL of acetylthiocholine chloride in a given concentration for assessment of Km and Vmax or 1 mM for toxicological and pharmacological investigations. Absorbance at 412 nm was measured immediately and after one minute. Enzyme activity was calculated estimating extinction coefficient $\varepsilon = 14{,}150\ M-1\ cm-1$. The oxime drugs were tested in a similar protocol. 425 μL of PBS was reduced to 325 μL of PBS. Paraoxon was added in concentration providing 95 % inhibition of AChE. Incubation time was set to 10 min. After that, 100 μL of oxime reactivator suspended in PBS was injected into the cuvette and kept for another 10 min. The reaction was started again by addition of acetylthiocholine.

Lactate concentration, and lactate dehydrogenase (LDH) and creatinine kinase (CK) activities in the serum and prefrontal cortex were assayed as markers of metabolic disruption. The activity of lactate

dehydrogenase (LDH) was assessed using a standard kit from Agappe Diagnostics Ltd., India. Initially, 1000 μL of working reagent and 10 μL of testicular homogenate were mixed and incubated at 37 °C for 1 min. Subsequently, the change in color absorbance (ΔOD/min) was measured every minute for a total of 3 min.

The activity of the enzyme was then calculated using the formula:

$$\text{LDH - P activity}(\text{U/L}) = (\Delta\text{OD/min}) \times 16030$$

This formula takes considers the change in absorbance over time and gives LDH activity in units per liter (U/L).

Plasma lactate levels were analyzed with a Lactate Colorimetric Assay Kit II (Bio Vision K627-100) and creatine kinase activities were measured using spectrophotometric method.

The concentrations of malondialdehyde (MDA) in the pre frontal cortex and hippocampus tissues were utilized as indicators of oxidative stress. MDA levels were determined through colorimetric methods based on the thiobarbituric acid method, measuring the thiobarbituric acid reactive substance (TBARS) generated during lipid peroxidation (Akhigbe and Ajayi, 2020), using standard laboratory kits from Oxford Biomedical Research, Inc., Oxford, USA. The concentration of lipid peroxidation was determined by quantifying the thiobarbituric acid reactive substances (TBARS) generated during the process, as previously described (Adegunlola et al., 2012). This method relies on the reaction between 2-thiobarbituric acid (TBA) and malondialdehyde, which is an end product of lipid peroxidation. Upon heating in acidic pH, a pink chromogen complex known as the [TBA]2-malondialdehyde adduct is formed and its absorbance is measured at 532 nm. In brief, 200 μL of the sample was deproteinized with 500 μL of Trichloroacetic acid (TCA) and centrifuged at 3000 rpm for 10 min. Then, 1 mL of 0.75 % TBA was added to 0.1 mL of the supernatant and boiled in a water bath for 20 min at 100 °C. The mixture was subsequently cooled with ice water. The absorbance of the sample/standard was then measured at 532 nm using a spectrophotometer against the blank. The concentration of TBARS generated was extrapolated from the standard curve.

The method described by Beutler et al. (Beutler et al., 1963) was employed to estimate the level of reduced glutathione (GSH). Initially, an aliquot of the sample was deproteinized by adding an equal volume of 4 % sulfosalicylic acid, followed by centrifugation at 4,000 rpm for 5 min. Subsequently, 0.5 mL of the supernatant was mixed with 4.5 mL of Ellman's reagent. A blank was prepared using 0.5 mL of the diluted precipitating agent and 4.5 mL of Ellman's reagent. The concentration of reduced glutathione, GSH, was determined by measuring the absorbance at 412 nm. This absorbance reading corresponds to the level of GSH present in the sample.

Catalase activity in both brain tissues was assessed following a previously established procedure Euler and Josephson (Euler and Josephson, 1927), with slight adaptations. Initially, 1 ml of the supernatant from the tissue homogenate was mixed with 19 mL of diluted water to achieve a 1:29 dilution of the sample. The assay mixture comprised 4 mL of H2O2 solution (800μmoles) and 5 ml of phosphate buffer in a 10 ml flat-bottom flask. Subsequently, 1 ml of appropriately diluted enzyme preparation was gently mixed with the reaction mixture by swirling at room temperature (37 °C). At 60-second intervals, 1 ml of the reaction mixture was extracted and introduced into 2 ml of dichromate/acetic acid reagent. The H2O2 content of the withdrawn sample was then determined. Catalase levels in the sample were quantified by comparing absorbance at 653 nm to that of a certified catalase standard.

Superoxide dismutase (SOD) activity was assessed following previously described protocols (Misra and Fridovich, 1972; Ige et al., 2011). Initially, 1 mL of the sample was diluted in 9 mL of distilled water to achieve a 1 in 10 dilution. Subsequently, 0.2 mL of the diluted sample was combined with 2.5 mL of 0.05 M carbonate buffer (pH 10.2) to allow for spectrophotometer equilibration. The reaction commenced upon the addition of 0.3 mL of freshly prepared 0.3 mM adrenaline to the mixture, which was promptly inverted for thorough mixing. In the reference cuvette, 2.5 mL of buffer, 0.3 mL of the substrate (adrenaline), and 0.2 mL of water were combined. The absorbance increase was monitored at 480 nm wavelength at 30-second intervals over a 150-second period.

The levels of TNF-α and IL-1β in the pre frontal cortex was assessed using a standard ELISA kits (Elabscience Biotechnology Co., Ltd, USA). Initially, 100 μL of both the standard and the sample were dispensed into individual wells, followed by a 90-minute incubation at 37 °C. Subsequently, the liquid was aspirated, and 100 μL of Biotinylated Detection Antibody Solution was added to each well, then incubated for 1 h at 37 °C. Afterward, the solution was aspirated and the wells were washed three times. Following this, 100 μL of HRP Conjugate was added to each well and incubated for 30 min at 37 °C. The solution was then aspirated from each well, and the wells were washed five times. Next, 90 μL of the substrate reagent was added to each well and incubated for 15 min at 37 °C. Finally, 50 μL of stop solution was added, and the optical density of each well was promptly read at 450 nm, with subsequent calculation of values.

Myeloperoxidase (MPO) activity, a marker of inflammatory cell infiltration (Akhigbe et al., 2021), was determined by colorimetry as earlier described by Desser et al. (Desser et al., 1972). Myeloperoxidase functions by oxidizing guaiacol to its oxidized state in the presence of hydrogen peroxide. The oxidized form of guaiacol exhibits a brown color, which was quantitatively assessed through photometric analysis at a wavelength of 470 nm. The intensity of the color produced is directly proportional to the concentration of oxidized guaiacol generated during the reaction.

Cysteine-aspartic proteases 3 (caspase 3) activities were quantified utilizing a standard ELISA kit (Elabscience Biotechnology Co., Ltd, USA), adhering to the manufacturer's instructions. Initially, the standard working solution was dispensed into the first two columns of the microplate, with each concentration added in duplicate to individual wells (50 μL per well). Samples were added to the remaining wells (50 μL per well). Subsequently, 50 μL of Biotinylated Detection Antibody working solution was promptly added to each well, and the plate was sealed with the provided sealer, then incubated for 45 min at 37 °C. Care was taken to ensure the solutions were added to the bottom of the wells, and measures were taken to minimize foaming and avoid touching the inner walls of the plate. Following incubation, the solution was aspirated from each well, and 350 μL of wash buffer was added to each well. The plate was soaked for 1–2 min, and the solution was then aspirated and the plate patted dry against clean absorbent paper. This washing step was repeated three times. Next, 100 μL of HRP Conjugate working solution was added to each well, followed by resealing the plate and incubating for 30 min at 37 °C. Subsequently, the solution was aspirated from each well, and the washing process was repeated five times. Then, 90 μL of Substrate Reagent was added to each well, the plate resealed, and incubated for an additional 15 min at 37 °C, while protecting the plate from light. After incubation, 50 μL of stop solution was added to each well, and the light density of each well was measured using a microplate reader set to 450 nm.

2.6. Histopathological assessment of the prefrontal cortex

The prefrontal cortex was fixed in 10 % formosaline. About 5 μm thick sections were obtained from paraffin blocks and stained with Haematoxylin and Eosin (H&E). Sections were also taken for Cresyl violet stains to assess the neurons. The sections were examined under a digital light microscope at various magnifications, then photomicrographs were taken at x 400 magnification.

The H&E-stained tissues were examined for atrophic neurons, pyknotic nuclei, inflammatory cell infiltration, and vascular congestion. The absence or presence of each of these lesions in about < 33 %, 33–66 %, and > 66 % of each slide from each animal was scored as 0, 1, 2, and 3 respectively (Ricken et al., 2023). The obtained photomicrographs from the Cresyl-stained tissues were imported to Image J for quantification of the normal pyramidal cell neurons. For histopathological evaluation, five sections were examined per slide of each animal. The mean of the

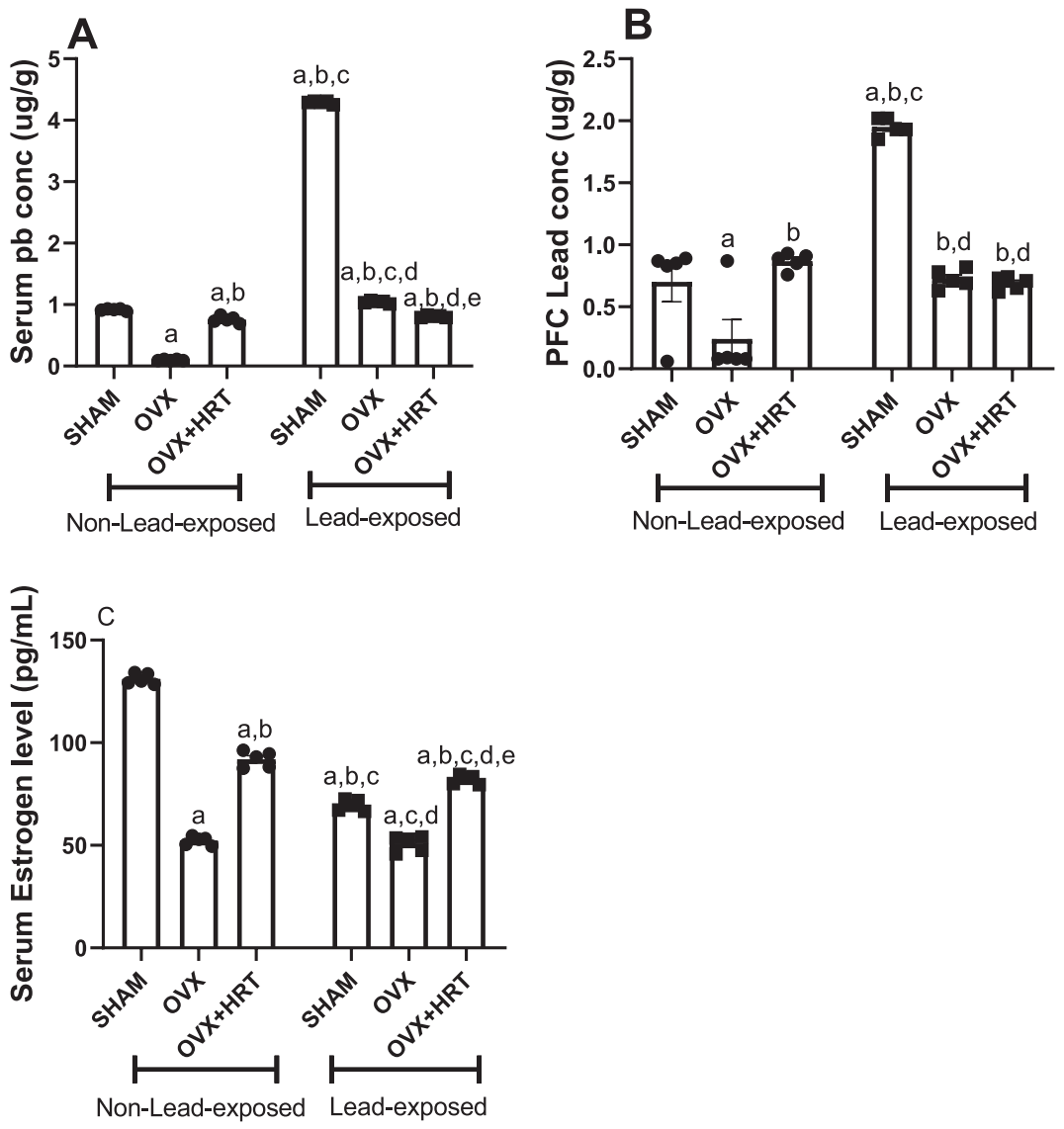

Fig. 1. Effects of hormone replacement therapy (HRT) on serum (A) and prefrontal cortex (PFC) (B) lead concentrations, and serum estrogen level (C) in lead-exposed ovariectomized (OVX) rats. $^{a}P < 0.05$ vs. Sham (non-lead-exposed), $^{b}P < 0.05$ vs. OVX (non-lead-exposed), $^{c}P < 0.05$ vs. OVX + HRT (non-lead-exposed), $^{d}P < 0.05$ vs.Sham (lead-exposed), $^{e}P < 0.05$ vs. OVX (lead-exposed).

values obtained for each group was normalized to control and reported. The pathologist who performed histopathological evaluation (H&E and Cresyl violet) was blinded to the study.

2.7. Statistical analysis

Data are reported as mean ± SEM. Statistical comparisons were made using two-way ANOVA, followed by Tukey's post hoc test for pairwise comparisons. Graph Pad Prism (version 5.0) was used for statistical analysis, with $p < 0.05$ indicating statistical significance.

3. Results

3.1. Effects of hormone replacement therapy on serum and prefrontal cortex lead concentration and estrogen level in lead-exposed ovariectomized rats

Lead exposure significantly increased serum lead concentration when compared with the sham-operated, ovariectomized, and HRT-treated ovariectomized rats. However, ovariectomized and HRT-treated ovariectomized rats showed significant reductions in serum lead concentration when compared to the sham-operated rats. Also, lead-exposed ovariectomized rat on HRT showed a marked reduction in serum lead concentration when compared with lead-exposed rats. Lead exposure significantly increased serum lead concentration. Also, HRT significantly reduced serum lead concentration. More so, there was a significant interaction between lead exposure and hormone status on serum lead concentration (Fig. 1A, Supplementary Table S1A). Furthermore, lead concentrations in sham-operated and ovariectomized rats were comparable. Nonetheless, it was significantly increased in OVX + HRT rats in comparison with the ovariectomized group. Lead exposure significantly increased lead concentration in the prefrontal cortex when compared with all other groups. Interestingly, ovariectomy and ovariectomy + HRT in lead-exposed rats significantly reduced lead concentration in the prefrontal cortex when compared with the lead-exposed rats. These findings also show that HRT improves lead concentration in the prefrontal cortex. Additionally, there was a significant interaction between lead exposure and hormone status on pre cortical lead concentration (Fig. 1B, Supplementary Table S1B).

Serum estrogen level was significantly reduced in ovariectomized

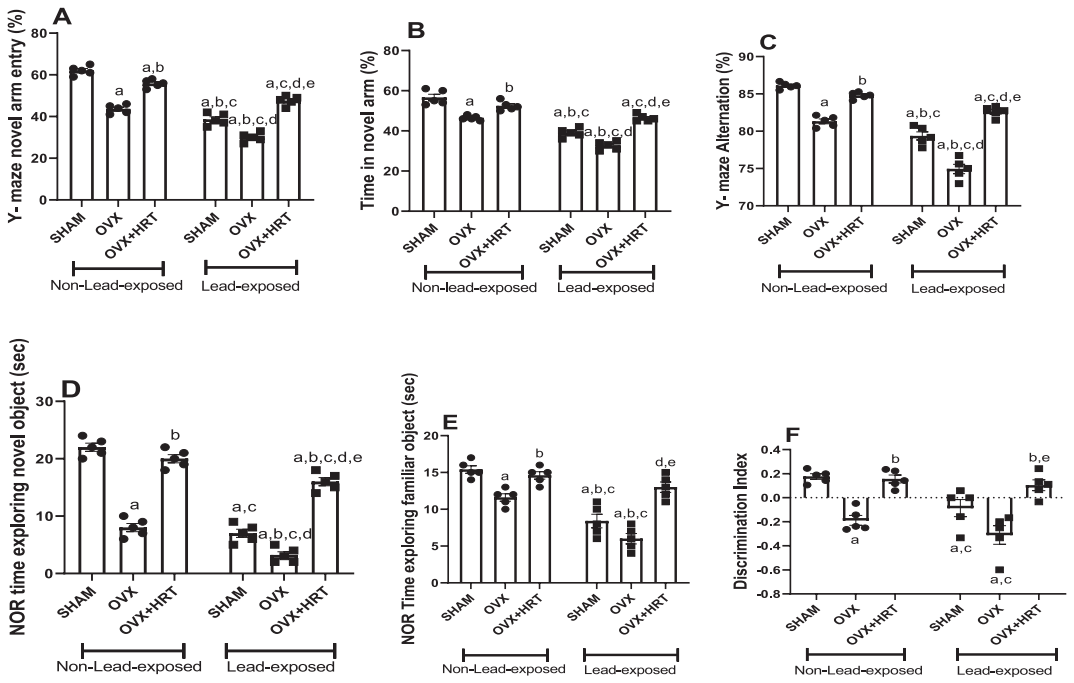

Fig. 2. Effects of hormone replacement therapy (HRT) on Y maze test findings viz. novel arm entry (A), time spent in novel arm (B), and alternation (C) and novel object recognition test viz. time exploring novel object (D), time exploring familiar object (E), and discrimination index (F) in lead-exposed ovariectomized (OVX) rats. $^{a}P < 0.05$ vs. Sham (non-lead-exposed), $^{b}P < 0.05$ vs. OVX (non-lead-exposed), $^{c}P < 0.05$ vs. OVX + HRT (non-lead-exposed), $^{d}P < 0.05$ vs. Sham (lead-exposed), $^{e}P < 0.05$ vs. OVX (lead-exposed).

animals when compared with the sham-operated rats. This reduction was attenuated by HRT in ovariectomized rats. In addition, lead exposure significantly reduced estrogen levels when compared with the sham-operated rats. When compared to sham, and lead-treated groups, lead exposure in ovariectomized rats also significantly reduced serum estrogen levels. HRT in ovariectomized lead-exposed rats significantly improved estrogen concentration when compared with lead-exposed and ovariectomized lead-exposed rats. These observations confirm that HRT significantly increased estrogen levels in lead exposed-ovariectomized rats. There was a significant interaction between lead exposure and hormone status on serum estrogen level (Fig. 1C, Supplementary Table S1C).

3.2. Effects of hormone replacement therapy on spatial memory cognition assessment in lead-exposed ovariectomized rats

Novel arm entry, the time spent in novel arm, and alternation were significantly reduced in ovariectomized rats when compared with the sham-operated rats. HRT improved these parameters in ovariectomized animals. In addition, lead exposure markedly reduced novel arm entry, the time spent in novel arm, and alternation, which were worsened by ovariectomy in lead-exposed rats when compared with the sham-operated. However, HRT improved these variables in lead-exposed ovariectomized rats when compared with lead-exposed rats and lead-exposed ovariectomized rats. In addition, there was significant interactions between lead exposure and hormone status on novel arm entry, time spent in novel arm and alternation (Fig. 2A-C, Supplementary Table S2A–C).

Furthermore, ovariectomy caused a significant reduction in the time spent exploring both novel and familiar objects and discrimination index when compared with the sham-operated rats. HRT improved these variables in ovariectomized animals. More so, lead exposure markedly reduced the time spent exploring both novel and familiar objects and discrimination index when compared with the sham-operated control animals. The reductions in these parameters observed in lead-exposed rats were aggravated by ovariectomy. Nonetheless, HRT significantly

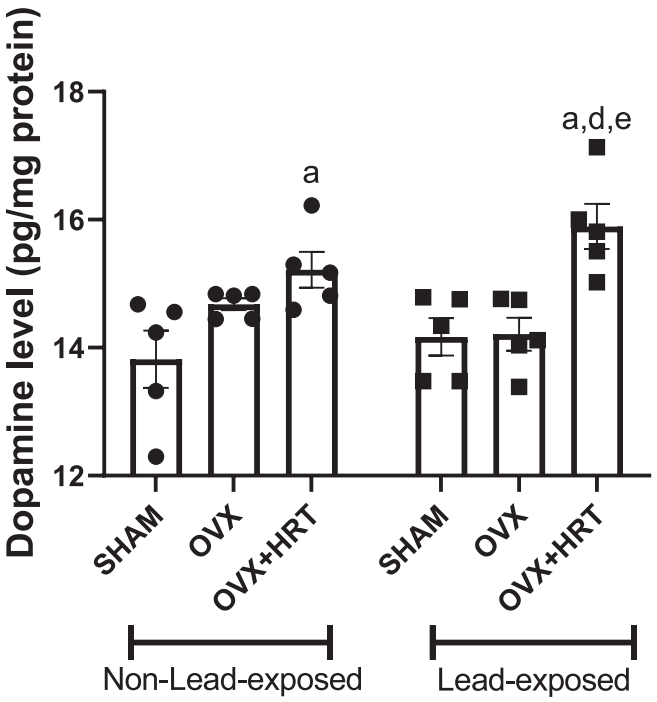

Fig. 3. Effects of hormone replacement therapy (HRT) on serum dopamine level in lead-exposed ovariectomized (OVX) rats. $^{a}P < 0.05$ vs. Sham (non-lead-exposed), $^{b}P < 0.05$ vs. OVX (non-lead-exposed), $^{c}P < 0.05$ vs. OVX + HRT(non-lead-exposed), $^{d}P < 0.05$ vs. Sham (lead-exposed), $^{e}P < 0.05$ vs. OVX (lead-exposed).

attenuated lead- and lead + ovariectomy-induced decline in the time spent exploring both novel and familiar objects and discrimination index. These findings demonstrate that ovariectomy worsens lead-induced decline in spatial memory and cognition, which may be

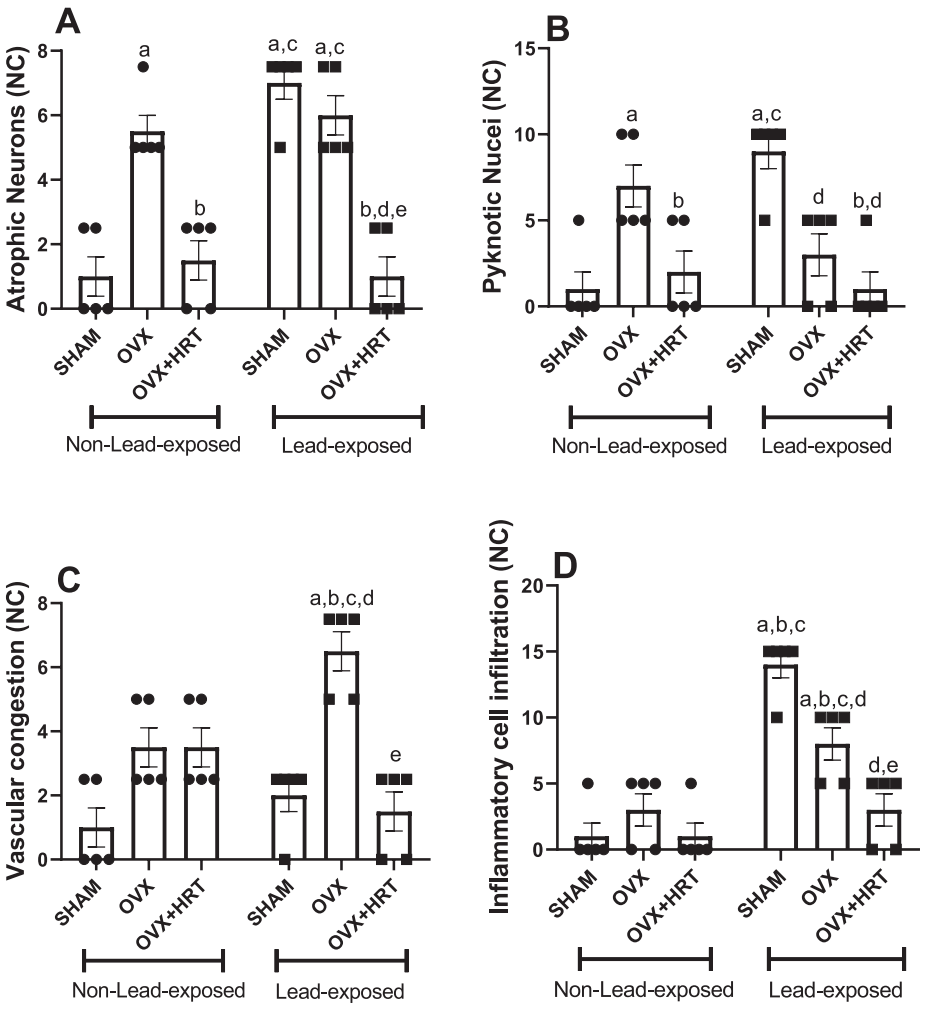

Fig. 4. Effects of hormone replacement therapy (HRT) on histopathological features of the prefrontal cortex (H&E, Mag.: x 400) viz: (A), Atrophic neurons (B), Pyknotic nuclei (C) Vascular congestion (D) Inflammatory cell infiltration in lead-exposed ovariectomized (OVX) rats. $^{a}P < 0.05$ vs. Sham (non-lead-exposed), $^{b}P < 0.05$ vs. OVX (non-lead-exposed), $^{c}P < 0.05$ vs. OVX + HRT(non-lead-exposed), $^{d}P < 0.05$ vs. Sham (lead-exposed), $^{e}P < 0.05$ vs. OVX (lead-exposed). Nr: neuropils; N: neuronal cells; G: glial cells; C: capillaries; black circle: focal area of inflammatory cell infiltration; star: focal areas of vascular congestions.

improved by HRT. In addition, there was a significant interaction between lead exposure and hormone status on time exploring novel object and time exploring familiar object but there is no significant interaction between lead exposure and hormone status on discrimination index (Fig. 2D-F, Supplementary Table S1D–F).

3.3. Effects of hormone replacement therapy on dopamine level in lead-exposed ovariectomized rats

Serum dopamine levels were comparable across the sham-operated, ovariectomized, and ovariectomized rats on HRT. However, lead exposure and ovariectomized lead-exposed rats had significantly reduced levels of dopamine when compared to the sham-operated, ovariectomized, and ovariectomized rats on HRT. The reduction in dopamine level in lead exposure and ovariectomized lead-exposed rats was ameliorated by HRT (Fig. 3). This reveals that lead exposure but not ovariectomy reduced dopamine level, which was improved by HRT. Serum dopamine levels were comparable across sham-operated, ovariectomized, lead exposed, and ovariectomized lead exposed rats. Dopamine levels increased significantly in ovariectomized rats on HRT in comparison to sham, and also increased in ovariectomized lead-exposed rats on HRT when compared with sham-operated, lead-exposed and ovariectomized-lead-exposed rats. In addition, there is no significant interaction between lead exposure and hormone status on dopamine levels (Fig. 3, Supplementary Table S3).

3.4. Effects of hormone replacement therapy on the histology of the prefrontal cortex and pyramidal neurons in lead-exposed ovariectomized rats

The prefrontal cortex of the sham-operated rats appears normal with normal neuropils and glial cells, and well-outlined neuronal cells. The capillaries also appear normal with no congestion. Ovariectomy led to the depletion of neuronal cells, and focal areas of inflammatory cell infiltration were seen. HRT improved the histology of the prefrontal cortex in ovariectomized rats. In addition, lead exposure caused the depletion of neuronal cells and focal areas of vascular congestions. The prefrontal cortex of the ovariectomized lead-exposed rats also appears distorted with depleted neuronal and glial cells, focal areas of vascular congestions within the capillaries, and focal areas of inflammatory cell infiltration. HRT improved the histology of the prefrontal cortex in ovariectomized lead-exposed rats (Fig. 4).

Severe atrophic neurons were observed in rats exposed to lead, while ovariectomized and lead-exposed ovariectomized rats showed moderate degree of atrophic neurons. Also, lead exposure caused a moderate degree of pyknotic nuclei, while ovariectomized rats showed mild levels of pyknosis. In addition, ovariectomized lead-exposed rats showed a moderate degree of inflammatory cell infiltration, while ovariectomized

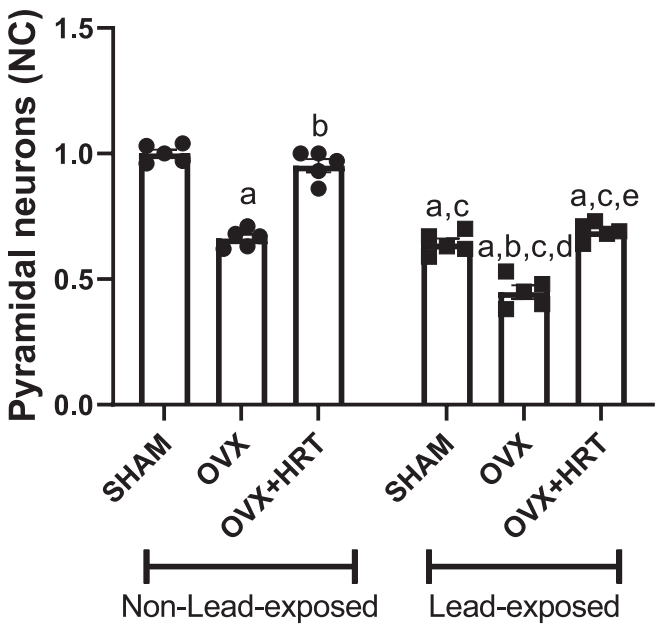

Fig. 5. Effects of hormone replacement therapy (HRT) on pyramidal neurons assessed by Cresyl violet stain in lead-exposed ovariectomized (OVX) rats (Mag.: x 400). $^{a}P < 0.05$ vs. Sham (non-lead-exposed), $^{b}P < 0.05$ vs. OVX (non-lead-exposed), $^{c}P < 0.05$ vs. OVX + HRT(non-lead-exposed), $^{d}P < 0.05$ vs. Sham (lead-exposed), $^{e}P < 0.05$ vs. OVX (lead-exposed). Photomicrograph of the prefrontal cortex (Cresyl violet stain, Mag: x400). The prefrontal cortex of the control rats appears normal with several normal pyramidal neurons (blue) that stained blue on Creysl violet stain. The prefrontal cortex of the ovariectomized rats appears distorted with few normal pyramidal neurons (blue) that stained blue on Creysl violet stain, and several pyknotic pyramidal neurons that appear pale (red). The prefrontal cortex of ovariectomized rats who had hormonal replacement therapy appears normal with several normal pyramidal neurons (blue) that stained blue on Creysl violet stain, and very few pyknotic pyramidal neurons that appear pale (red). Lead exposure caused distorted prefrontal cortex with few normal pyramidal neurons (blue) that stained blue on Creysl violet stain, and several pyknotic pyramidal neurons that appear pale (red). The prefrontal cortex of ovariectomized lead-exposed rats appears distorted with very few normal pyramidal neurons (blue) that stained blue on Creysl violet stain, and several pyknotic pyramidal neurons that appear pale (red). The prefrontal cortex of ovariectomized lead-exposed rats who had hormone replacement therapy appears normal with several normal pyramidal neurons (blue) that stained blue on Creysl violet stain, and few pyknotic pyramidal neurons that appear pale (red). (For interpretation of the references to color in this figure legend, the reader is referred to the web version of this article.)

rats and ovariectomized rats on HRT showed only a mild degree of inflammatory cell infiltration. Furthermore, lead exposure led to a severe degree of vascular congestion. There was a significant increase in atrophic neurons in ovariectomized, lead-exposed and ovariectomized lead-exposed rats when compared with sham, this was improved by HRT in ovariectomized rats and ovariectomized lead-exposed rats. Pyknotic nuclei also increased significantly in ovariectomized rats and lead exposed rats when compared with sham non-lead-exposed which was attenuated by HRT. Vascular congestion is comparable across sham non-lead-exposed, ovariectomized, ovariectomized rats on HRT as well as lead exposed rats. Meanwhile, there is a significant increase in vascular congestion in ovariectomized lead-exposed rats when compared with sham, ovariectomized, ovariectomized on HRT as well as lead-exposed rats, this was attenuated by HRT in ovariectomized lead-exposed rats. Inflammatory cell infiltration was comparable across sham-operated, ovariectomized and ovariectomized rats on HRT but increased significantly in lead-exposed and ovariectomized lead-exposed rats when compared with sham, ovariectomized, and ovariectomized rats on HRT. HRT improves inflammatory cell infiltration in ovariectomized lead-exposed rats. In addition, there were significant interactions between lead exposure and hormone status on atrophic neurons, pyknotic nuclei, vascular congestion and inflammatory cell infiltration (Fig. 4A-D, Supplementary Table S4A–D).

In comparison with the sham-operated rats, normal pyramidal neurons were significantly reduced in ovariectomized rats, which was improved by HRT. Also, lead exposure markedly reduced the expression of normal pyramidal neurons, which was worsened by ovariectomy in lead-exposed rats, when compared with the sham-operated control rats. The decline in normal pyramidal neurons was attenuated by HRT in ovariectomized lead-exposed rats. However, there was a significant interaction between lead exposure and hormone status on pyramidal neurons (Fig. 5, Supplementary Table S5).

3.5. Effects of hormone replacement therapy on markers of metabolic disruption in lead-exposed ovariectomized rats

Lactate concentration was significantly increased in the serum but decreased in the prefrontal cortex in ovariectomized rats when compared with the sham-operated rats. This alteration was attenuated by HRT. Also, lead exposure significantly increased lactate levels in the serum and prefrontal cortex, which was worsened in ovariectomized lead-exposed rats, when compared with the sham-operated, ovariectomized, and ovariectomized rats on HRT. Lead- and ovariectomized lead-exposure-induced rise in lactate content was attenuated by HRT. Furthermore, LDH and CK activities were markedly increased in the serum and prefrontal cortex in ovariectomized rats when compared with the sham-operated rats. HRT improved ovariectomy-induced upsurge in LDH and CK activities in the serum and prefrontal cortex. Lead exposure led to a marked rise in LDH and CK activities, which was aggravated in ovariectomized lead-exposed rats but attenuated in ovariectomized lead-exposed rats on HRT when compared with the sham-operated rats. These findings show that ovariectomy and lead exposure induce metabolic disruptions, which may be attenuated by HRT. Additionally, there was significant interactions between lead exposure and hormone status on lactate level, LDH and CK activities in the serum and prefrontal cortex (Fig. 6A–F, Supplementary Table S6A–F).

3.6. Effects of hormone replacement therapy on oxidative stress markers in lead-exposed ovariectomized rats

Ovariectomy led to an increase in MDA content in the prefrontal content when compared with the sham-operated rats. Nonetheless, HRT suppressed the rise in MDA levels in ovariectomized rats. Also, in comparison with other groups, lead exposure significantly increased MDA levels in the prefrontal cortex which was worsened in ovariectomized lead-exposed rats. The rise in MDA level observed in the ovariectomized lead-exposed rats was attenuated by HRT. In addition, there was a significant interaction between lead exposure and hormone status on MDA levels in the prefrontal cortex (Fig. 7A, Supplementary Table S7A).

Furthermore, ovariectomy led to a decline in GSH level as well as SOD and catalase activities in the prefrontal content when compared with the sham-operated rats. However, HRT attenuated the decline in GSH level, and SOD and catalase activities induced by ovariectomy. When compared with the sham-operated rats, lead exposure significantly downregulated GSH levels, and SOD and catalase activities, which was worsened in ovariectomized lead-exposed rats. The decline in GSH level and SOD and catalase activities observed in the ovariectomized lead-exposed rats was attenuated by HRT. Also, there was significant interactions between lead exposure and hormone status on GSH level, SOD and catalase activities in the prefrontal cortex (Fig. 7B–D, Supplementary Table S7B–D).

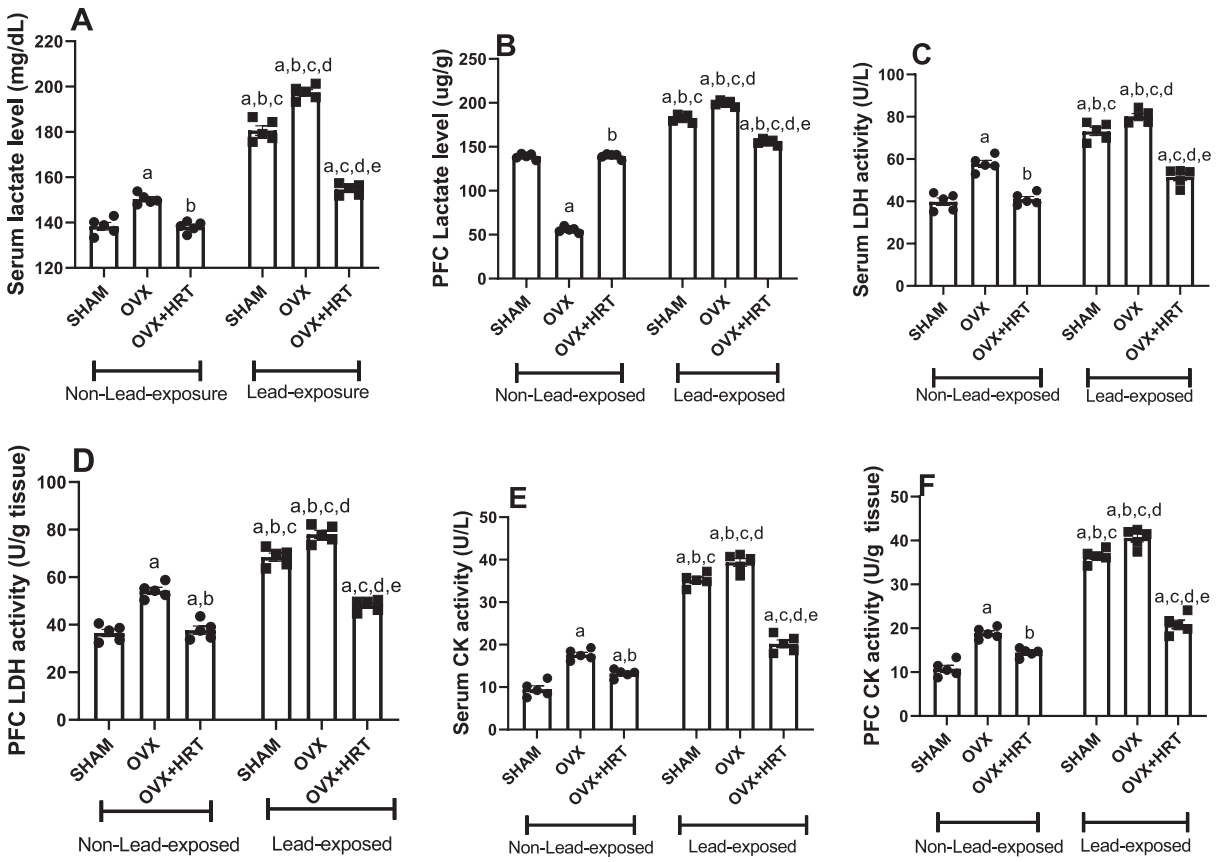

Fig. 6. Effects of hormone replacement therapy (HRT) on serum (A) and prefrontal cortex (B) lactate level, serum (C) and prefrontal cortex (D) lactate dehydrogenase (LDH) activities, and serum (E) and prefrontal cortex (F) creatinine kinase (CK) activities in lead-exposed ovariectomized (OVX) rats. $^{a}P < 0.05$ vs. Sham (non-lead-exposed), $^{b}P < 0.05$ vs. OVX (non-lead-exposed), $^{c}P < 0.05$ vs. OVX + HRT (non-lead-exposed), $^{d}P < 0.05$ vs. Sham (lead-exposed), $^{e}P < 0.05$ vs. OVX (lead-exposed).

3.7. Effects of hormone replacement therapy on inflammatory and apoptotic markers in lead-exposed ovariectomized rats

MPO activity and TNF-α and IL-1β levels were significantly increased in ovariectomized rats when compared with sham-operated rats. The observed rise in these inflammatory markers in ovariectomized animals was significantly ameliorated by HRT. Also, lead exposure significantly increased these inflammatory markers in the prefrontal cortex when compared to the sham-operated, ovariectomized, and ovariectomized rats on HRT. Ovariectomized lead exposure led to a significant rise in MPO activity and IL-1β, but not TNF-α, when compared with lead-exposed rats. HRT significantly attenuated the rise in MPO activity and TNF-α and IL-1β levels in ovariectomized lead-exposed rats. In addition, there were significant interactions between lead exposure and hormone status on MPO activity, TNF-α and IL-1β levels in the prefrontal cortex (Fig. 8A–C, Supplementary Table S8A–C).

Additionally, ovariectomy and lead exposure caused a significant rise in caspase 3 activity in the prefrontal cortex when compared with the sham-operated, ovariectomized, and ovariectomized rats on HRT. HRT significantly attenuated ovariectomy + lead-induced rise in caspase 3 activity. Also, there was a significant interaction between lead exposure and hormone status on caspase 3 activity in the prefrontal cortex (Fig. 8D, Supplementary Table S8D).

4. Discussion

The present findings that lead concentrations in the serum and prefrontal cortex increased significantly agree with previous studies that lead concentration increases not just in the serum but in tissues following lead exposure (Nascimento et al., 2016; Andjelkovic et al., 2019); Besong et al., 2023a). The observed rise in lead concentration in the prefrontal cortex may explain the associated decline in estrogen levels following lead exposure. Exposure to lead causes hormonal imbalances through the suppression of the hypothalamic-pituitary axis, leading to decreased responses to stimulation of thyrotropin-releasing hormone, growth hormone-releasing hormone, and gonadotropin-releasing hormone and reduced growth hormone, follicle-stimulating hormone (FSH), luteinizing hormone (LH) and estrogen (Firoozichahak et al., 2022). Although it is a known fact that HRT increases circulating estrogen levels, the present study confirms this and also provides additional evidence demonstrating that HRT does not only improve estrogen levels, it reduces the lead concentrations in the serum and prefrontal cortex. This may have been due to the fact that estrogen plays an essential role in the absorption and distribution of lead (Firoozichahak et al., 2022; Wang et al., 2022; Zhang et al., 2023).

Exposure to lead in post-menopausal state, induced by ovariectomy, independently caused a deficit in spatial memory evidenced by reduced novel arm entry, time spent in the novel arm, reduced time exploring novel and familiar objects, and decreased alternation and discrimination index. Although this is similar to previous studies that showed that lead exposure caused cognitive deficits (Yu et al., 2019; Chulikhit et al., 2021; Baek et al., 2024), and earlier studies that documented that estrogen decline in the post-menopausal state is a potential trigger for cognitive deficit (Schmidt et al., 2015). This seems to be the first study to report that lead exposure in postmenopausal state (which was induced by ovariectomy in this study) leads to cognitive deficit. Hence, the present findings form an extension of the available data in the literature demonstrating that menopause-induced spatial memory loss and

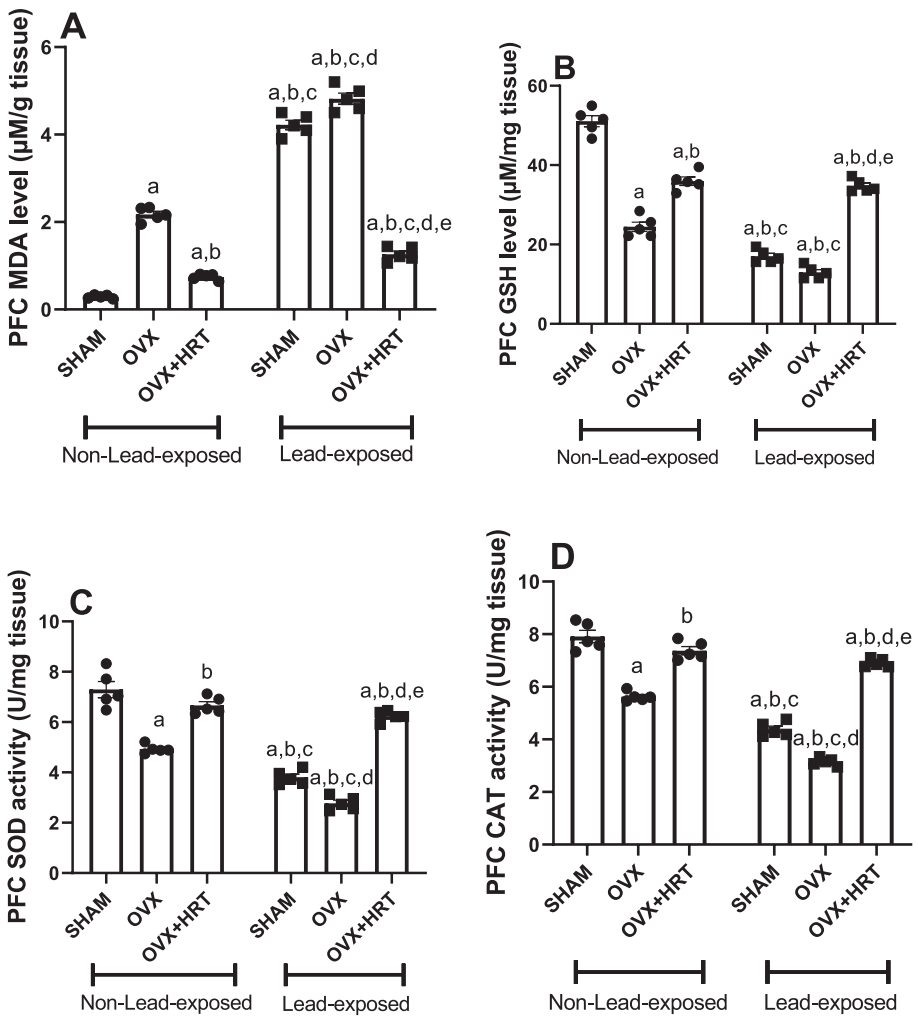

Fig. 7. Effects of hormone replacement therapy (HRT) on prefrontal cortex (PFC) malondialdehyde, MDA, (A) and reduced glutathione, GSH, (B) levels and superoxide, SOD, (C) and catalase (D) activities in lead-exposed ovariectomized (OVX) rats. $^{a}P < 0.05$ vs. Sham (non-lead-exposed), $^{b}P < 0.05$ vs. OVX (non-lead-exposed), $^{c}P < 0.05$ vs. OVX + HRT(non-lead-exposed), $^{d}P < 0.05$ vs. Sham (lead-exposed), $^{e}P < 0.05$ vs. OVX (lead-exposed).

cognitive deficit may be aggravated in lead exposure.

It is likely that the post-menopausal state and lead-exposure-induced spatial memory deficit are mediated not just by estrogen-dependent mechanism but also by a decline in dopamine level. Lead exposure in ovariectomized rats caused in decline in dopamine concentration, possibly by inhibiting the release of GABA and dopamine triggered by Ca-KCl (Weisskopf et al., 2010). However, our present finding that HRT improves lead-induced spatial memory loss and cognition deficit in ovariectomized rats was accompanied by increased dopamine concentration. This agrees with previous report of Lokuge et al. (Lokuge et al., 2010) that estrogen confers neuroprotection by modulating neurotransmitter production, neuronal development, synapse establishment, density of neuronal spines, and neural signal transmission. This finding suggest that HRT improved spatial memory and cognition in ovariectomized lead-exposed rats by upregulating dopamine release.

In an attempt to explore the involvement of other mechanisms apart from dopaminergic signaling that may influence the adverse effects of lead exposure and ovariectomy on spatial memory, lactate level, and LDH and CK activities were assessed as indices of tissue injury and metabolic disruption. Post-menopausal state with lead exposure induce metabolic disruption and tissue injury evidenced by increased LDH and CK activities, and lactate concentration. LDH promotes the reversible conversion of lactate to pyruvate and in a pathological state, metabolic disruption is associated with an enhanced LDH activity which distorts the electron transport chain, lowers ATP generation, and increases lactate production (Barbosa et al., 2021). CK facilitates the reversible conversion of creatine to phosphocreatine, an easily transportable energy source. Brain CK is known to supply ATPases with phosphocreatine locally and to sustain ATP levels in regions where oxygen or nutrient availability is restricted, and where metabolic function and phosphocreatine regeneration are either partially or completely compromised (Schlattner et al., 2016). Hence, the present findings that lead exposure in post-menopausal state increased lactate levels which was accompanied by a rise in CK and LDH activities show that lead and post-menopausal state independently impaired metabolic function and reduced energy generation for neuronal activities in the prefrontal cortex.

In the physiological state, there are leakages of electrons during the electron transport chain in the mitochondria which contributes to the physiological levels of free radicals (Indo *et al.*, 2007); however, in pathological conditions, the released electrons are in excess leading to increased generation of reactive oxygen species, ROS (Tabassum et al., 2020). It is likely that the lead exposure in post-menopausal state induced metabolic disruption and promoted ROS generation, resulting in oxidative injury of the prefrontal cortex as depicted by a rise in MDA that was accompanied by a decline in GSH, SOD, and catalase activities. These agree with the findings of Chulikhit et al. (Chulikhit et al., 2021) that revealed that ovariectomy causes motor dysfunction via the induction of oxidative stress and those of Leão et al. (Leão et al., 2021) that demonstrated that lead exposure causes neurodegeneration by

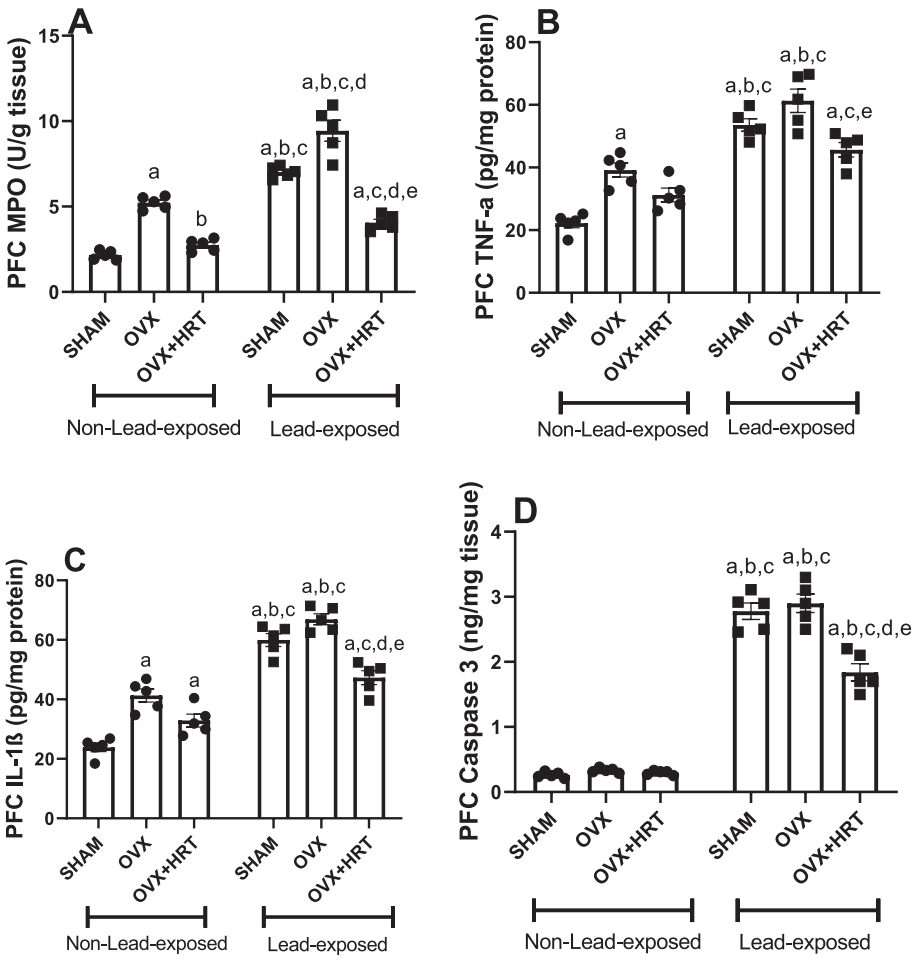

Fig. 8. Effects of hormone replacement therapy (HRT) on prefrontal cortex (PFC) myeloperoxidase (MPO) activity (A), tumour necrotic factor-alpha (TNF-α) (B), interleukin-1beta (IL-1β) (C), and caspase 3 activity (D) in lead-exposed ovariectomized (OVX) rats. $^{a}P < 0.05$ vs. Sham (non-lead-exposed), $^{b}P < 0.05$ vs. OVX (non-lead-exposed), $^{c}P < 0.05$ vs. OVX + HRT(non-lead-exposed), $^{d}P < 0.05$ vs. Sham (lead-exposed), $^{e}P < 0.05$ vs. OVX (lead-exposed).

promoting oxidative stress. Notwithstanding, the protective effect of HRT on spatial memory and cognition in lead-exposed ovariectomized rats may be mediated, at least in part, via the suppression of oxidative stress. The present findings that HRT led to the downregulation of MDA and upregulation of GSH level and SOD and catalase activities agrees with the study of Ventura-Clapier et al. (Ventura-Clapier et al., 2017) that reported that HRT exerts antioxidant activities possibly due to its phenolic ring structure. Estrogen may also suppress ROS-driven oxidative stress by maintaining cellular metabolic bioenergetics and redox equilibrium (Torres et al., 2018; Klinge, 2020).

A growing body of research suggests that inflammation may be a cause or result of oxidative damage (Akhigbe et al., 2024). Our findings that lead exposure in ovariectomized led to increased MPO activities and pro-inflammatory cytokines like TNF-α and IL-1β in association with oxidative stress reveal that the inflammatory process observed may be due to the oxidative stress induced by these states. Ovariectomy and lead exposure likely activates NF-κB which leads to the transcription of these pro-inflammatory cytokines, causing the inflammation of the prefrontal cortex (Huang et al., 2017). In agreement with studies that document that estrogen replacement therapy inhibits the generation and release of pro-inflammatory cytokines (Khan et al., 2021) and neuroinflammation associated with menopause (Wang et al., 2020), the present study observed that HRT suppressed MPO activity, and TNF-α and IL-1β. This may be attributed to the suppression of oxidative stress by HRT as well as the possible downregulation of inducible nitric oxide synthase (iNOS) and cyclooxygenase-2 (COX-2) expression (Villa et al., 2016) which leads to reduced TNF-α and IL-1β. Previous studies have reported that lead exposure (Wu et al., 2021) and ovariectomy (Ge et al., 2020) independently activates microglial cells to mediate inflammatory injury in the prefrontal cortex. Hence, in agreement with the report of Wang et al. (Wang et al., 2021), it is likely that HRT inhibited the activation of microglial cells, thus suppressing neuroinflammation induced by lead exposure and ovariectomy.

Oxidative stress and inflammation are established triggers of caspase 3-mediated apoptosis, a programmed cell death that is mediated through the intrinsic and extrinsic pathways (Okoh et al., 2020). Our present findings suggest that lead exposure in ovariectomized rats upregulated caspase 3 activity possibly by promoting the translocation of cytochrome *c* into the cytoplasm, leading to the binding of Cytochrome *C* with apoptotic protease activating factor-1 (Apaf-1) and formation of an apoptosome, which in turn activates caspase 9 that initiates the cleaving and activation of pro-caspase-3/7, ultimately resulting in apoptosis (Sun et al., 2017). The initiation of caspase 3-mediated apoptosis in lead-exposed ovariectomized rats might be through the induction of oxidative stress and inflammation. The observed cascade of pathophysiological processes in lead-exposed ovariectomized rats was accompanied by distortions of the histology of the prefrontal cortex, notably depletion of neuronal cells, inflammatory cell infiltration, vascular congestion, and increased number of pyknotic pyramidal nuclei and atrophic neurons. This corroborates the report of Samy et al. (Samy et al., 2023) in ovariectomized rats. Interestingly, HRT alleviated caspase 3 upregulation and distortions in prefrontal cortical histology, possibly by suppressing oxidative stress and inflammation, thus preventing the translocation of cytochrome *C* into the cytosol and

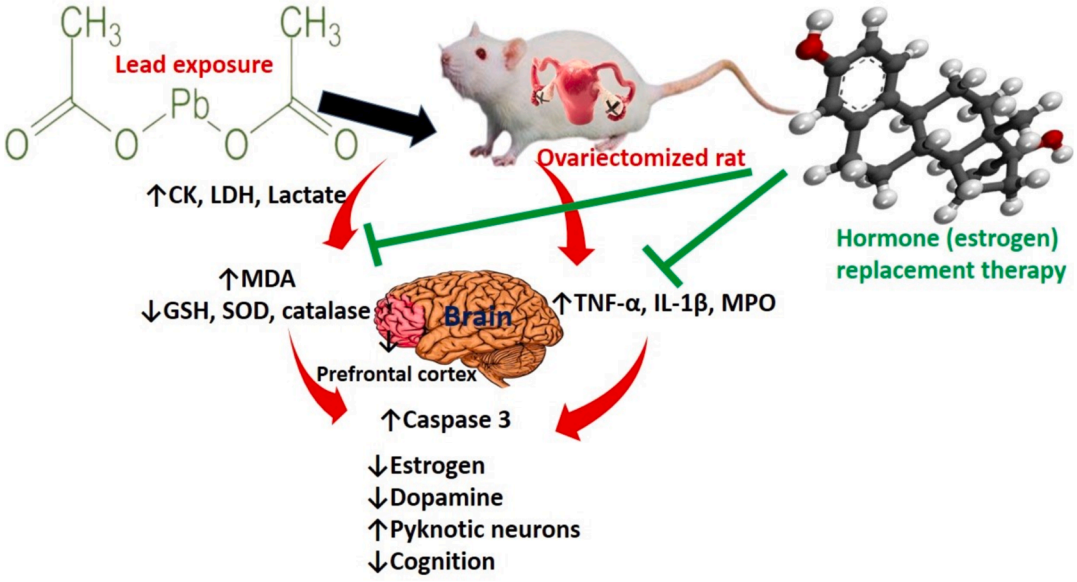

Fig. 9. Schematic illustration of the effect of hormone replacement therapy on cognition and pyramidal neurons in the prefrontal cortex in lead-exposed ovariectomized rats.

activation of caspase 3.

5. Conclusion

Summing up, lead exposure in menopausal state (as demonstrated by ovariectomized lead-exposed rats) may cause pyramidal cell neurodegeneration and memory loss via multiple pathways, including downregulation of estrogen and dopamine, metabolic disruption, oxido-inflammation, and apoptosis. However, HRT attenuated ovariectomized/lead exposure-induced neurodegeneration and spatial memory loss through the upregulation of estrogen and dopamine levels, and suppressing of metabolic disruption, oxidative stress, inflammation, and apoptosis (Fig. 9). Further studies exploring other possible mechanisms of postmenopausal state and/or lead exposure-induced spatial memory loss and neurodegeneration are recommended. This will unravel novel therapeutic opportunities in the management of cognition deficits associated with menopause and lead exposure.

Funding

N/A.

Declaration of competing interest

The authors declare that they have no known competing financial interests or personal relationships that could have appeared to influence the work reported in this paper.

Acknowledgment

N/A. The study was self funded.

Ethical Approval

The study was approved by the Ethics Review Committee of the Faculty of Basic Medical Sciences, Ladoke Akintola University of Technology. Ogbomoso, Oyo State, Nigeria (ERCFBMSLAUTECH: 042/06/2024).

Appendix A. Supplementary data

Supplementary data to this article can be found online at https://doi.org/10.1016/j.crtox.2024.100200.

Data availability

Data will be made available on request.

References

Adegunlola, J.G., Afolabi, O.K., Akhigbe, R.E., Adegunlola, G.A., Adewumi, O.M., Oyeyipo, I.P., Ige, S.F., Afolabi, A.O., 2012. Lipid peroxidation in brain tissue following administration of low and high doses of arsenite and L-ascorbate in Wistar strain rats. Toxicol. Int. 19 (1), 47.

Adeyanju, O.A., Soetan, O.A., Soladoye, A.O., Olatunji, L.A., 2018. Oral hormonal therapy with ethinylestradiol–levonorgestrel improves insulin resistance, obesity, and glycogen synthase kinase-3 independent of circulating mineralocorticoid in estrogen-deficient rats. Can. J. Physiol. Pharmacol. 96 (6), 577–586.

Afolabi, O.A., Hamed, M.A., Anyogu, D.C., Adeyemi, D.H., Odetayo, A.F., Akhigbe, R.E., 2022. Atorvastatin-mediated downregulation of VCAM-1 and XO/UA/caspase 3 signaling averts oxidative damage and apoptosis induced by ovarian ischaemia/reperfusion injury. Redox Rep. 27 (1), 212–220.

Akhigbe, R., Ajayi, A., 2020. Testicular toxicity following chronic codeine administration is via oxidative DNA damage and up-regulation of NO/TNF-α and caspase 3 activities. PLoS One 15 (3), e0224052.

Akhigbe, R.E., Ajayi, L.O., Ajayi, A.F., 2021. Codeine exerts cardiorenal injury via upregulation of adenine deaminase/xanthine oxidase and caspase 3 signaling. Life Sci. 273, 118717.

Akhigbe, R.E., Aminat, B.O.A., Akhigbe, T.M., Hamed, M.A., 2024. Glutamine Alleviates I/R-Induced Intestinal Injury and Dysmotility Via the Downregulation of Xanthine Oxidase/Uric Acid Signaling and Lactate Generation in Wistar Rats. J. Surg. Res. 295, 431–441.

Ambikairajah, A., Walsh, E., Cherbuin, N., 2022. A review of menopause nomenclature. Reprod. Health 19 (1), 29.

Andjelkovic, M., Buha Djordjevic, A., Antonijevic, E., Antonijevic, B., Stanic, M., Kotur-Stevuljevic, J., Spasojevic-Kalimanovska, V., Jovanovic, M., Boricic, N., Wallace, D., Bulat, Z., 2019. Toxic effect of acute cadmium and lead exposure in rat blood, liver, and kidney. Int. J. Environ. Res. Public Health 16 (2), 274.

Andy, C., Nerattini, M., Jett, S., Carlton, C., Zarate, C., Boneu, C., Fauci, F., Ajila, T., Battista, M., Pahlajani, S., Christos, P., 2024. Systematic review and meta-analysis of the effects of menopause hormone therapy on cognition. Front. Endocrinol. 15, 1350318.

Baek, D.C., Kang, J.Y., Lee, J.S., Lee, E.J., Son, C.G., 2024. Linking alterations in estrogen receptor expression to memory deficits and depressive behavior in an ovariectomy mouse model. Sci. Rep. 14 (1), 6854.

Barbosa, J., Faria, J., Garcez, F., Leal, S., Afonso, L.P., Nascimento, A.V., Moreira, R., Pereira, F.C., Queirós, O., Carvalho, F., Dinis-Oliveira, R.J., 2021. Repeated administration of clinically relevant doses of the prescription opioids tramadol and

tapentadol causes lung, cardiac, and brain toxicity in Wistar rats. Pharmaceuticals 14 (2), 97.
Besong, E.E., Ashonibare, P.J., Obembe, O.O., Folawiyo, M.A., Adeyemi, D.H., Hamed, M.A., Akhigbe, T.M., Akhigbe, R.E., 2023a. Zinc protects against lead-induced testicular damage via modulation of steroidogenic and xanthine oxidase/uric acid/caspase 3-mediated apoptotic signaling in male Wistar rats. Aging Male 26 (1), 2224428.
Besong, E.E., Akhigbe, T.M., Ashonibare, P.J., Oladipo, A.A., Obimma, J.N., Hamed, M. A., Adeyemi, D.H., Akhigbe, R.E., 2023b. Zinc improves sexual performance and erectile function by preventing penile oxidative injury and upregulating circulating testosterone in lead-exposed rats. Redox Rep. 28 (1), 2225675.
Beutler, E., Duron, O., Kelly, B.M., 1963. Improved method for the determination of blood glutathione. J Lab Clin Med 61, 882–888.
Bjørklund, G., Tippairote, T., Hangan, T., Chirumbolo, S., Peana, M., 2024. Early-life lead exposure: risks and neurotoxic consequences. Curr. Med. Chem. 31 (13), 1620–1633.
Bu, J., Liu, Y., Zhang, R., Lin, S., Zhuang, J., Sun, L., Zhang, L., He, H., Zong, R., Wu, Y., Li, W., 2024. Potential New Target for Dry Eye Disease—Oxidative Stress. Antioxidants 13 (4), 422.
Bustamante-Barrientos, F.A., Méndez-Ruette, M., Ortloff, A., Luz-Crawford, P., Rivera, F. J., Figueroa, C.D., Molina, L., Bátiz, L.F., 2021. The impact of estrogen and estrogen-like molecules in neurogenesis and neurodegeneration: beneficial or harmful? Front. Cell. Neurosci. 15, 636176.
Chaudhary, S., Kumaran, S.S., Goyal, V., Kalaivani, M., Kaloiya, G.S., Sagar, R., Mehta, N., Srivastava, A.K., Jagannathan, N.R., 2021. Frontal lobe metabolic alterations characterizing Parkinson's disease cognitive impairment. Neurol. Sci. 42, 1053–1064.
Cheng, Y.J., Lin, C.H., Lane, H.Y., 2021. From menopause to neurodegeneration—molecular basis and potential therapy. Int. J. Mol. Sci. 22 (16), 8654.
Chulikhit, Y., Sukhano, W., Daodee, S., Putalun, W., Wongpradit, R., Khamphukdee, C., Umehara, K., Noguchi, H., Matsumoto, K., Monthakantirat, O., 2021. Effects of Pueraria candollei var mirifica (Airy Shaw and Suvat.) Niyomdham on ovariectomy-induced cognitive impairment and oxidative stress in the mouse brain. Molecules 26 (11), 3442.
Desser RK, Himmelhoch SR, Evans WH, Januska M, Mage M, and Shelton E. Arch. Biochem. Biophys.1972, 148, 452–465 pmid:4623114.
Echeverria, V., Echeverria, F., Barreto, G.E., Echeverría, J., Mendoza, C., 2021. Estrogenic plants: to prevent neurodegeneration and memory loss and other symptoms in women after menopause. Front. Pharmacol. 12, 644103.
Ellington, K., Link, T., Saccomano, S.J., 2022. Menopause: A primary care perspective. Nurse Pract. 47 (2), 16–23.
Euler, H.V., Josephson, K., 1927. Über katalase I. Justus Liebigs Annalen Der Chemie 452 (1), 158–181.
Firoozichahak, A., Rahimnejad, S., Rahmani, A., Parvizimehr, A., Aghaei, A., Rahimpoor, R., 2022. Effect of occupational exposure to lead on serum levels of lipid profile and liver enzymes: An occupational cohort study. Toxicol. Rep. 9, 269–275.
Ge, F., Yang, H., Lu, W., Shi, H., Chen, Q., Luo, Y., Liu, L., Yan, J., 2020. Ovariectomy Induces Microglial Cell Activation and Inflammatory Response in Rat Prefrontal Cortices to Accelerate the Chronic Unpredictable Stress-Mediated Anxiety and Depression. Biomed Res. Int. 2020 (1), 3609758.
Giannini, A., Caretto, M., Genazzani, A.R. and Simoncini, T., 2021. Neuroendocrine changes during menopausal transition. Endocrines, 2(4), pp.405-416.
Goney, M.P., Wilce, M.C., Wilce, J.A., Stocker, W.A., Goodchild, G.M., Chan, K.L., Walton, K.L., 2020. Engineering the ovarian hormones inhibin A and inhibin B to enhance synthesis and activity. Endocrinology 161 (8), bqaa099.
Gudadhe, S., Singh, S.K., Ahsan, J., 2024. Cellular and Neurological Effects of Lead (Pb) Toxicity. In: Lead Toxicity Mitigation: Sustainable Nexus Approaches. Cham, Springer Nature Switzerland, pp. 125–145.
Hammond, T.R., Marsh, S.E., Stevens, B., 2019. Immune signaling in neurodegeneration. Immunity 50 (4), 955–974.
Hirano, S., 2021. Clinical implications for dopaminergic and functional neuroimage research in cognitive symptoms of Parkinson's disease. Mol. Med. 27 (1), 40.
Huang, W.Y., Hsin, I.L., Chen, D.R., Chang, C.C., Kor, C.T., Chen, T.Y., Wu, H.M., 2017. Circulating interleukin-8 and tumor necrosis factor-α are associated with hot flashes in healthy postmenopausal women. PLoS One 12 (8), e0184011.
Iantomasi, T., Romagnoli, C., Palmini, G., Donati, S., Falsetti, I., Miglietta, F., Aurilia, C., Marini, F., Giusti, F., Brandi, M.L., 2023. Oxidative stress and inflammation in osteoporosis: molecular mechanisms involved and the relationship with microRNAs. Int. J. Mol. Sci. 24 (4), 3772.
Ige, S.F., Akhigbe, R.E., Adewale, A.A., Badmus, J.A., Olaleye, S.B., Ajao, F.O., Saka, W. A., Owolabi, O.Q., 2011. Effect of Allium cepa (Onion) Extract on cadmium induced nephrotoxicity in rats. Kidney Res J 1 (1), 41–47.
Jee, D., Park, S.H., Hwang, H.S., Kim, H.S., Kim, M.S., Kim, E.C., 2021. Effects of hormone replacement therapy on lens opacity, serum inflammatory cytokines, and antioxidant levels. Ann. Med. 53 (1), 707–714.
Kang, S., Lee, J., Choi, S., Nesbitt, J., Min, P.H., Trushina, E. and Choi, D.S., 2023. Moderate ethanol exposure reduces astrocyte-induced neuroinflammatorysignaling and cognitive decline in presymptomatic APP/PS1 mice.
Khan, I., Saeed, K., Jo, M.G., Kim, M.O., 2021. 17-β estradiol rescued immature rat brain against glutamate-induced oxidative stress and neurodegeneration via regulating Nrf2/HO-1 and MAP-kinase signaling pathway. Antioxidants 10 (6), 892.
Klinge, C.M., 2020. Estrogenic control of mitochondrial function. Redox Biol. 31, 101435.
Kurtishi, A., Rosen, B., Patil, K.S., Alves, G.W., Møller, S.G., 2019. Cellular proteostasis in neurodegeneration. Mol. Neurobiol. 56, 3676–3689.
Leão, L.K.R., Bittencourt, L.O., Oliveira, A.C.A., Nascimento, P.C., Ferreira, M.K.M., Miranda, G.H.N., de Oliveira Ferreira, R., Eiró-Quirino, L., Puty, B., Dionizio, A. and Cartágenes, S.C., 2021. Lead-induced motor dysfunction is associated with oxidative stress, proteome modulation, and neurodegeneration in motor cortex of rats. Oxidative Medicine and Cellular Longevity, 2021.
Levine, L., Hall, J.E., 2023. Does the environment affect menopause? A review of the effects of endocrine disrupting chemicals on menopause. Climacteric 26 (3), 206–215.
Lokuge, S., Frey, B.N., Foster, J.A., Soares, C.N., Steiner, M., 2010. The rapid effects of estrogen: a mini-review. Behav. Pharmacol. 21 (5–6), 465–472.
London, E.D., 2020. Human brain imaging links dopaminergic systems to impulsivity. Recent Advances in Research on Impulsivity and Impulsive Behaviors, pp.53-71.
Misra, H.P., Fridovich, I., 1972. The role of superoxide anion in the autoxidation of epinephrine and a simple assay for superoxide dismutase. J. Biol. Chem. 247 (10), 3170–3175.
Mohamad, N.V., Ima-Nirwana, S. and Chin, K.Y., 2020. Are oxidative stress and inflammation mediators of bone loss due to estrogen deficiency? A review of current evidence. Endocrine, Metabolic & Immune Disorders-Drug Targets (Formerly Current Drug Targets-Immune, Endocrine & Metabolic Disorders), 20(9), pp.1478-1487.
Nascimento, C.R.B., Risso, W.E., dos Reis Martinez, C.B., 2016. Lead accumulation and metallothionein content in female rats of different ages and generations after daily intake of Pb-contaminated food. Environ. Toxicol. Pharmacol. 48, 272–277.
Nunes, E., Gallardo, E., Morgado-Nunes, S., Fonseca-Moutinho, J., 2024. Postmenopausal Cognitive Function and Steroid Hormone Levels. J Reprod Med Gynecol Obstet 9 (166), 2.
Okoh, L., Ajayi, A.M., Ben-Azu, B., Akinluyi, E.T., Emokpae, O., Umukoro, S., 2020. d-Ribose–l-cysteine exhibits adaptogenic-like activity through inhibition of oxido-inflammatory responses and increased neuronal caspase-3 activity in mice exposed to unpredictable chronic mild stress. Mol. Biol. Rep. 47, 7709–7722.
Ortega, D.R., Esquivel, D.F.G., Ayala, T.B., Pineda, B., Manzo, S.G., Quino, J.M., Mora, P. C., de la Cruz, V.P., 2021. Cognitive impairment induced by lead exposure during lifespan: Mechanisms of lead neurotoxicity. Toxics 9 (2).
Ricken, A.M., Hamed, M.A., Akhigbe, R.E., 2023. Histopathological evaluation of infertility: Lessons from laboratory rodents. Histol. Histopathol. 18684.
Sabbatini, A.R., Kararigas, G., 2020. Menopause-related estrogen decrease and the pathogenesis of HFpEF: JACC review topic of the week. J. Am. Coll. Cardiol. 75 (9), 1074–1082.
Samy, D.M., Mostafa, D.K., Saleh, S.R., Hassaan, P.S., Zeitoun, T.M., Ammar, G.A., Elsokkary, N.H., 2023. Carnosic acid mitigates depression-like behavior in ovariectomized mice via activation of Nrf2/HO-1 pathway. Mol. Neurobiol. 60 (2), 610–628.
Santoro, N., Roeca, C., Peters, B.A., Neal-Perry, G., 2021. The menopause transition: signs, symptoms, and management options. J. Clin. Endocrinol. Metab. 106 (1), 1–15.
Schirinzi, T., Canevelli, M., Suppa, A., Bologna, M., Marsili, L., 2020. The continuum between neurodegeneration, brain plasticity, and movement: a critical appraisal. Rev. Neurosci. 31 (7), 723–742.
Schlattner, U., Klaus, A., Ramirez Rios, S., Guzun, R., Kay, L., Tokarska-Schlattner, M., 2016. Cellular compartmentation of energy metabolism: creatine kinase microcompartments and recruitment of B-type creatine kinase to specific subcellular sites. Amino Acids 48, 1751–1774.
Schmidt, P.J., Dor, R.B., Martinez, P.E., Guerrieri, G.M., Harsh, V.L., Thompson, K., Koziol, D.E., Nieman, L.K., Rubinow, D.R., 2015. Effects of estradiol withdrawal on mood in women with past perimenopausal depression: a randomized clinical trial. JAMA Psychiat. 72 (7), 714–726.
Sharma, A., Davies, R., Kapoor, A., Islam, H., Webber, L., Jayasena, C.N., 2023. The effect of hormone replacement therapy on cognition and mood. Clin. Endocrinol. 98 (3), 285–295.
Stute, P., Wienges, J., Koller, A.S., Giese, C., Wesemüller, W., Janka, H., Baumgartner, S., 2021. Cognitive health after menopause: does menopausal hormone therapy affect it? Best Pract. Res. Clin. Endocrinol. Metab. 35 (6), 101565.
Sun, D.K., Wang, L., Zhang, P., 2017. Antitumor effects of chrysanthemin in PC-3 human prostate cancer cells are mediated via apoptosis induction, caspase signalling pathway and loss of mitochondrial membrane potential. Afr. J. Tradit. Complement. Altern. Med. 14 (4), 54–61.
Tabassum, N., Kheya, I.S., Asaduzzaman, S., Maniha, S., Fayz, A.H., Zakaria, A., Noor, R., 2020. A review on the possible leakage of electrons through the electron transport chain within mitochondria. Life Sci 6, 105–113.
Tanbo, T.G., Fedorcsak, P.Z., 2021. Can time to menopause be predicted? Acta obstetricia et gynecologica Scandinavica 100 (11), 1961–1968.
Taylor, W.D., Zald, D.H., Felger, J.C., Christman, S., Claassen, D.O., Horga, G., Miller, J. M., Gifford, K., Rogers, B., Szymkowicz, S.M., Rutherford, B.R., 2022. Influences of dopaminergic system dysfunction on late-life depression. Mol. Psychiatry 27 (1), 180–191.
Torres, M.J., Kew, K.A., Ryan, T.E., Pennington, E.R., Lin, C.T., Buddo, K.A., Fix, A.M., Smith, C.A., Gilliam, L.A., Karvinen, S., Lowe, D.A., 2018. 17β-Estradiol directly lowers mitochondrial membrane microviscosity and improves bioenergetic function in skeletal muscle. Cell Metab. 27 (1), 167–179.
Ventura-Clapier, R., Moulin, M., Piquereau, J., Lemaire, C., Mericskay, M., Veksler, V., Garnier, A., 2017. Mitochondria: a central target for sex differences in pathologies. Clin. Sci. 131 (9), 803–822.
Villa, A., Vegeto, E., Poletti, A., Maggi, A., 2016. Estrogens, neuroinflammation, and neurodegeneration. Endocr. Rev. 37 (4), 372–402.
Virgolini, M.B. and Aschner, M., 2021. Molecular mechanisms of lead neurotoxicity. In Advances in neurotoxicology (Vol. 5, pp. 159-213). Academic Press.

Vrachnis, N., Zygouris, D., Vrachnis, D., Antonakopoulos, N., Fotiou, A., Panagopoulos, P., Kolialexi, A., Pappa, K., Mastorakos, G., Iliodromiti, Z., 2021. Effects of hormone therapy and flavonoids capable on reversal of menopausal immune senescence. Nutrients 13 (7), 2363.

Wang, Y., Mishra, A. and Brinton, R.D., 2020. Transitions in metabolic and immune systems from pre-menopause to post-menopause: implications for age-associated neurodegenerative diseases. F1000Research, 9.

Wang, J., Hou, Y., Zhang, L., Liu, M., Zhao, J., Zhang, Z., Ma, Y., Hou, W., 2021. Estrogen attenuates traumatic brain injury by inhibiting the activation of microglia and astrocyte-mediated neuroinflammatory responses. Mol. Neurobiol. 58, 1052–1061.

Wang, B., Zhang, W., Chen, C., Chen, Y., Xia, F., Wang, N., Lu, Y., 2022. Lead exposure and impaired glucose homeostasis in Chinese adults: a repeated measures study with 5 years of follow-up. Ecotoxicol. Environ. Saf. 243, 113953.

Weisskopf, M.G., Weuve, J., Nie, H., Saint-Hilaire, M.H., Sudarsky, L., Simon, D.K., Hersh, B., Schwartz, J., Wright, R.O., Hu, H., 2010. Association of cumulative lead exposure with Parkinson's disease. Environ. Health Perspect. 118 (11), 1609–1613.

Witkowska, D., Słowik, J., Chilicka, K., 2021. Heavy metals and human health: Possible exposure pathways and the competition for protein binding sites. Molecules 26 (19), 6060.

Wu, L., Li, S., Pang, S., Zhang, B., Wang, J., He, B., Lv, L., Wang, W., Zhao, N., Zhang, Y., 2021. Effects of lead exposure on the activation of microglia in mice fed with high-fat diets. Environ. Toxicol. 36 (9), 1923–1931.

Xu, Q., Li, D., Chen, J., Yang, J., Yan, J., Xia, Y., Zhang, F., Wang, X., Cao, H., 2022. Crosstalk between the gut microbiota and postmenopausal osteoporosis: Mechanisms and applications. Int. Immunopharmacol. 110, 108998.

Yu, M., D'Hooge, R. and Van der Jeugd, A., 2019, May. Functional deficits in menopause-associated encephalopathy: a behavioural rodent study. In Front. Neurosci. Conference Abstract: 13th National Congress of the Belgian Society for Neuroscience. doi: 10.3389/conf. fnins (Vol. 43).

Zhang, W., Cui, Y. and Liu, J., 2023. The association between blood heavy metals level and sex Virgolini p.1175011.

Zhang, W.Y., Guo, Y.J., Wang, K.Y., Chen, L.M., Jiang, P., 2020. Neuroprotective effects of vitamin D and 17ß-estradiol against ovariectomy-induced neuroinflammation and depressive-like state: Role of the AMPK/NF-κB pathway. Int. Immunopharmacol. 86, 106734.

Zhang, Z., Yu, J., Xie, J., Liu, D., Fan, Y., Ma, H., Wang, C., Hong, Z., 2021. Improvement roles of zinc supplementation in low dose lead induced testicular damage and glycolytic inhibition in mice. Toxicology 462, 152933.